Supplement of:

Drainage reorganization induces deviations in width-area-slope scaling of valleys and channels

Elhanan Harel et al.

Correspondence to: Elhanan Harel (elhnananh@post.bgu.ac.il)

S1 Algorithm for identifying optimal locations for width measurements

This section describes the semi-automatic ArcGIS-based algorithm for measuring valley width. The algorithm input is a valley bottom (VBET) polygon, and the output is a set of width measurement locations and values.

1. A network of valley centerlines is defined for the valley bottom polygon (Fig. S1) by applying the external ArcGIS tool 'polygon to centerline' (Dilts, 2015). Valley center points are distributed along the centerline at distances ranging between 5-20 m for small and large basins, respectively.

2. Thiessen (Voronoi) polygons are created around the centerline points and clipped based on the extent of the VBET polygon (Fig. S2A).

3. Intersecting edges of Thiessen polygons are eliminated (Fig. S2B). The remaining edges, which are sub-perpendicular to the centerlines, cross the VBET polygon from side to side, and are far from valley confluences and bends, are defined as 'crossing Thiessen lines.'

4. Steps 2-3 are repeated twice more (overall three iterations). In each iteration, the centerlines are trimmed relative to the previous iteration, such that in each iteration, the minimal valley order (sensu Strahler) included in the centerline network is higher. The second and third iterations are designated to increase the number of 'crossing Thiessen lines' along the high order valleys: At the end of the first iteration, 'crossing Thiessen lines' are generated along valleys of all orders. In the second iteration, new 'crossing Thiessen lines' are generated along second and higher order valleys, and so on in the third iteration. When a new 'crossing Thiessen line' intersects a 'crossing Thiessen line' that was generated in a previous iteration, the new line is eliminated. Finally, 'crossing Thiessen lines' from all three iterations are merged into a single shapefile (Fig. S3). In the current study, three iterations were sufficient to generate 'crossing Thiessen lines' in basins with high order valleys. However, future use of this method for basins with valley order >5 should consider additional iterations.

5. Centerline segments that are bounded between pairs of 'crossing Thiessen lines' that were adjacent to each other prior to step 3, are defined as 'Width-locator segments,' and their midpoints are marked (Fig. S4). Following, 'Width transects' are generated perpendicular to the 'width-locator segments'. 'Width transects' cross through the midpoints and terminate at the edges of the valley bottom polygon (Fig. S4). 'Width transects' are generated by applying the external ArcGIS 'Create perpendicular lines tool' (Gabrish, 2020), and their length represent the local valley width (Fig. 3A).

7. Finally, the 'intersection points' between the 'Width transects' and the valley talweg (flowlines) are marked (Fig. S5). Drainage area and topographic data used for slope calculation are extracted at the 'intersection points,' based on the TanDEM-X 0.4 arcsec DEM (Wessel, 2016).

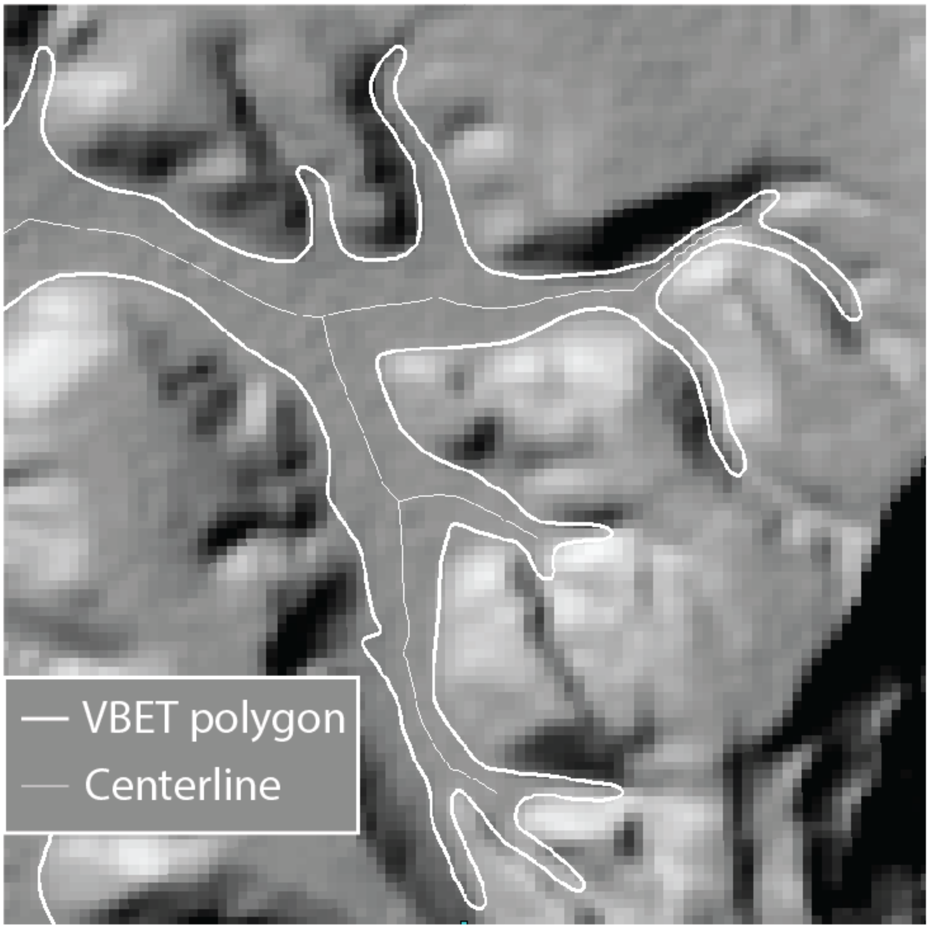

Figure S1. The VBET polygon (thick lines) and its centerline (thin lines). The current and following examples are based on the basin containing valley 4, and the hillshade backgrounds are based on TanDEM-X 0.4 arcsec DEM (Wessel, 2016)

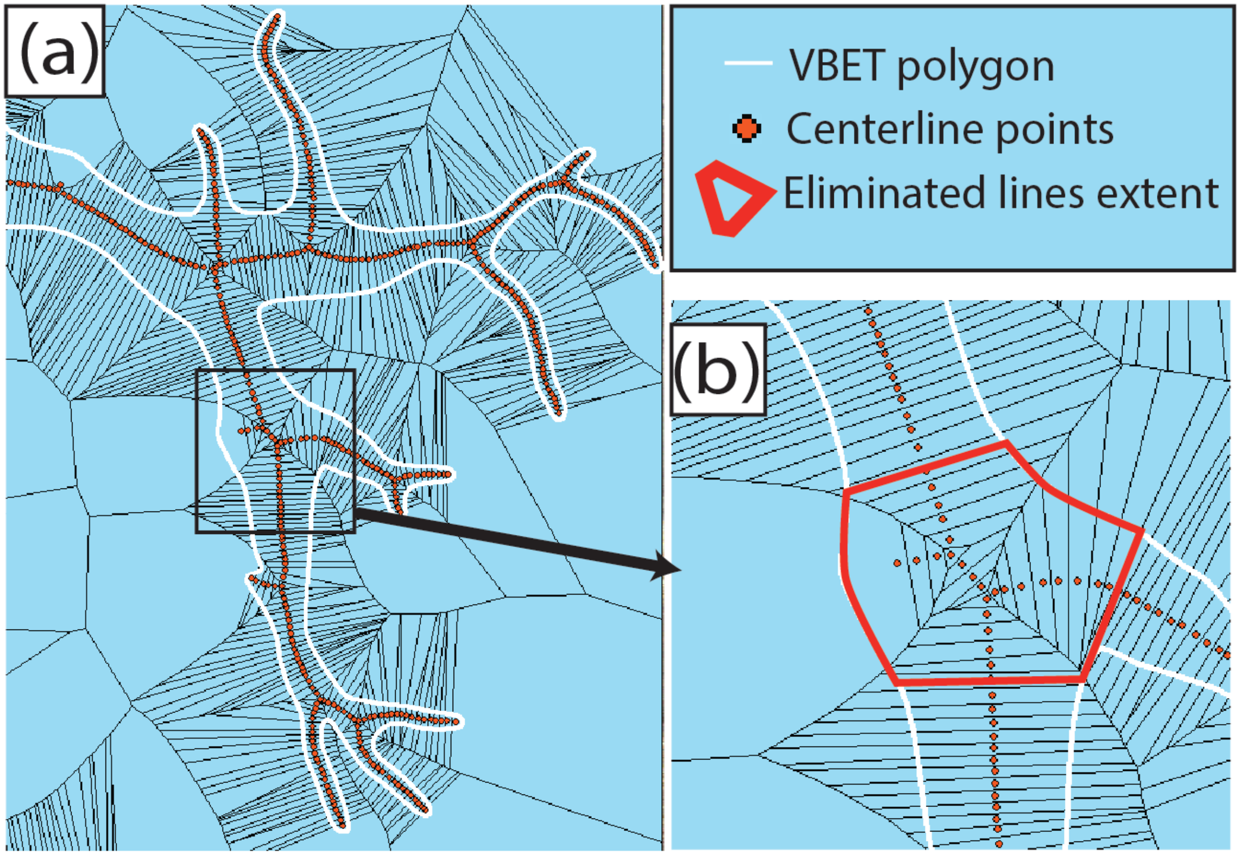

Figure S2 (a) Thiessen polygons (black) around centerline points (red). In step 2, the polygons are maintained only within the VBET boundaries (white). (b) In step 3, intersecting edges of Thiessen polygons are eliminated (e.g., within the red polygon area).

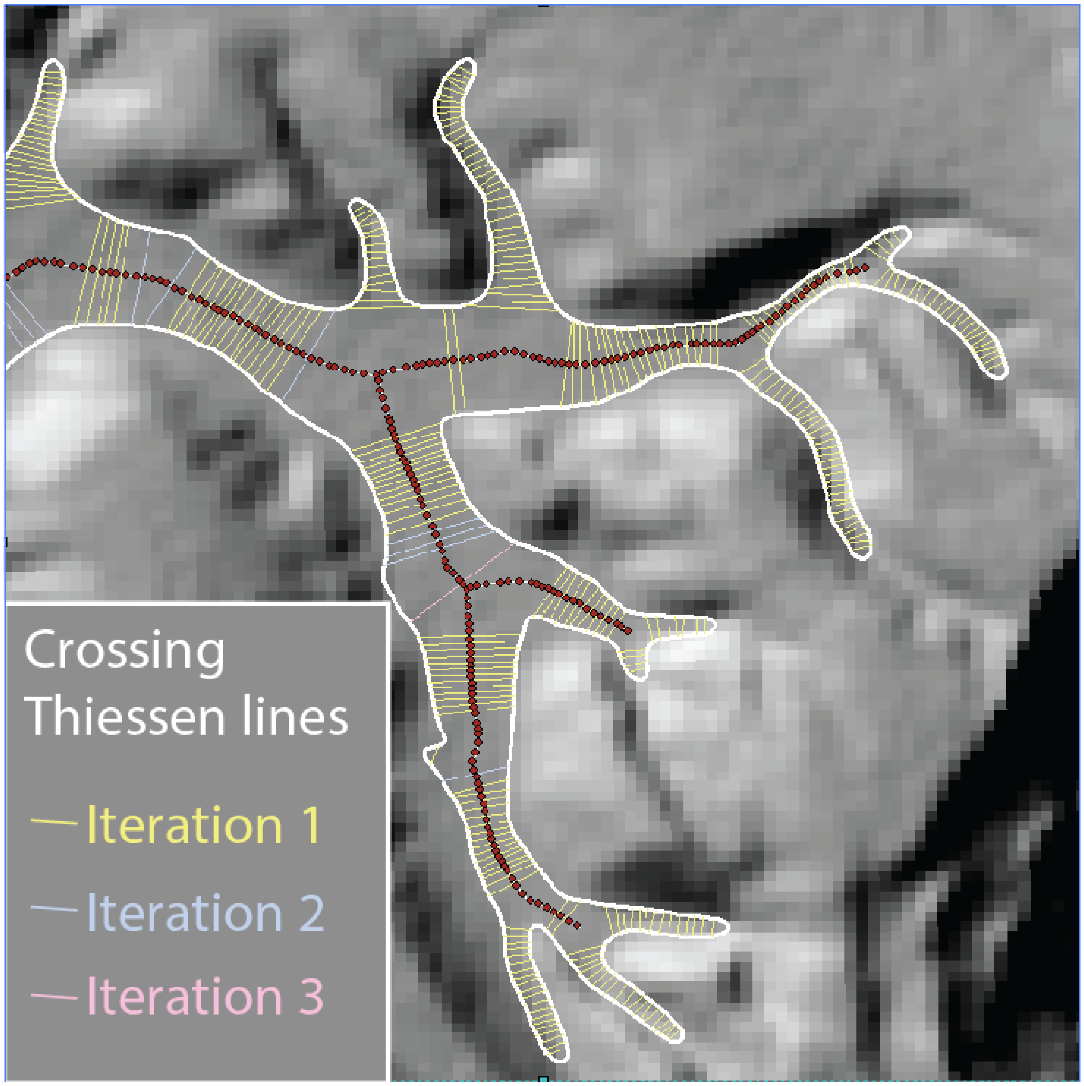

Figure S3: 'Crossing Thiessen lines' compiled from the three iterations described in step 4.

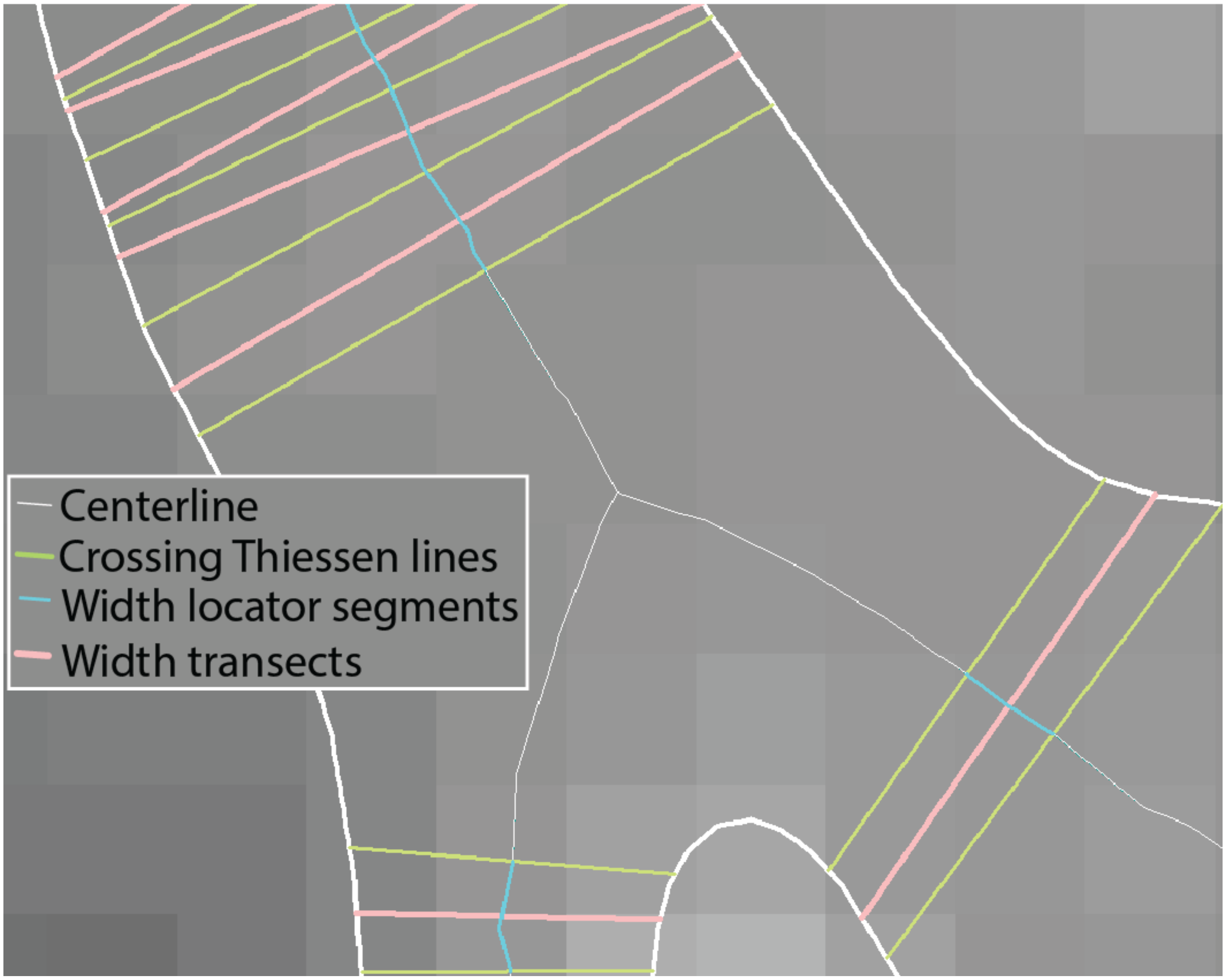

Figure S4: 'Width locator segments' (turquoise) are defined between pairs of originally adjacent 'Crossing Thiessen lines' (Green). Then, 'Width transects' (pink), whose lengths represent the valley width, are generated perpendicular and at the midpoints of the 'Width locator segments.'

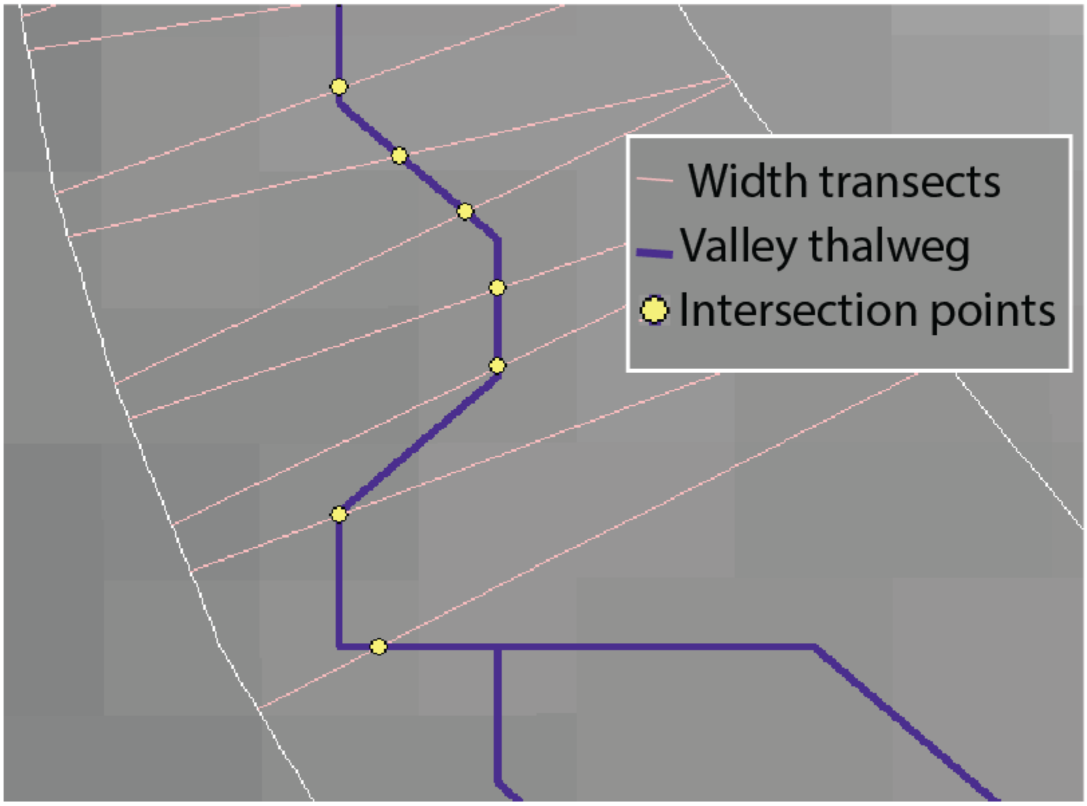

Fig. S5: Intersection points (yellow) are defined along intersections between 'Width transects' (pink) and the thalweg (blue), as part of step 6.

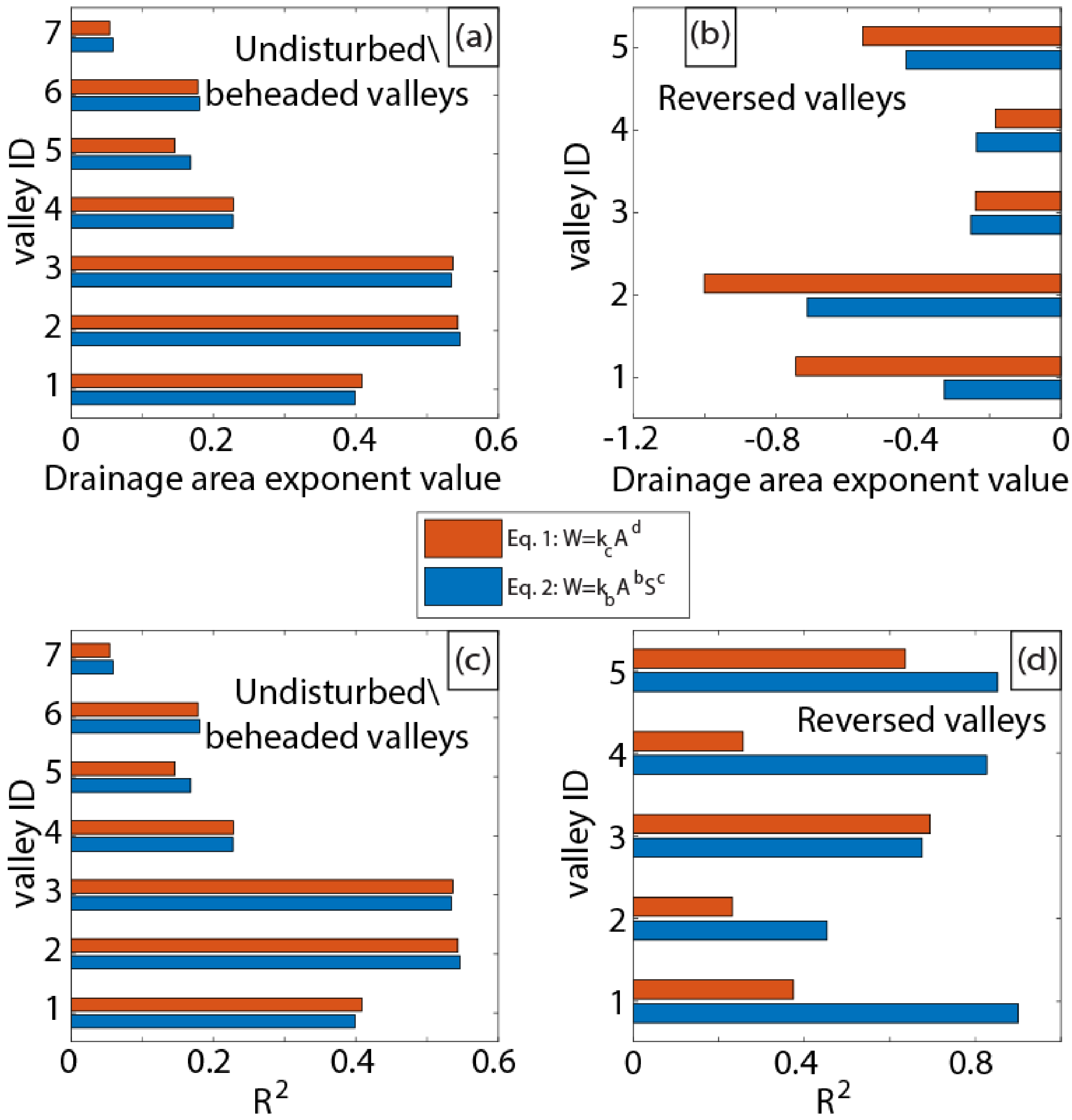

Figure S6: A comparison between the area exponents and R^2 values based on equations 1 and 2. In the undisturbed and beheaded valleys in panels (a) and (c), the best-fit exponent values have no meaningful difference, and the R^2 is similar. In contrast, in the reversed valleys, the two models predict different exponents (b), and the R^2 values are higher when using Eq. 2 (d).

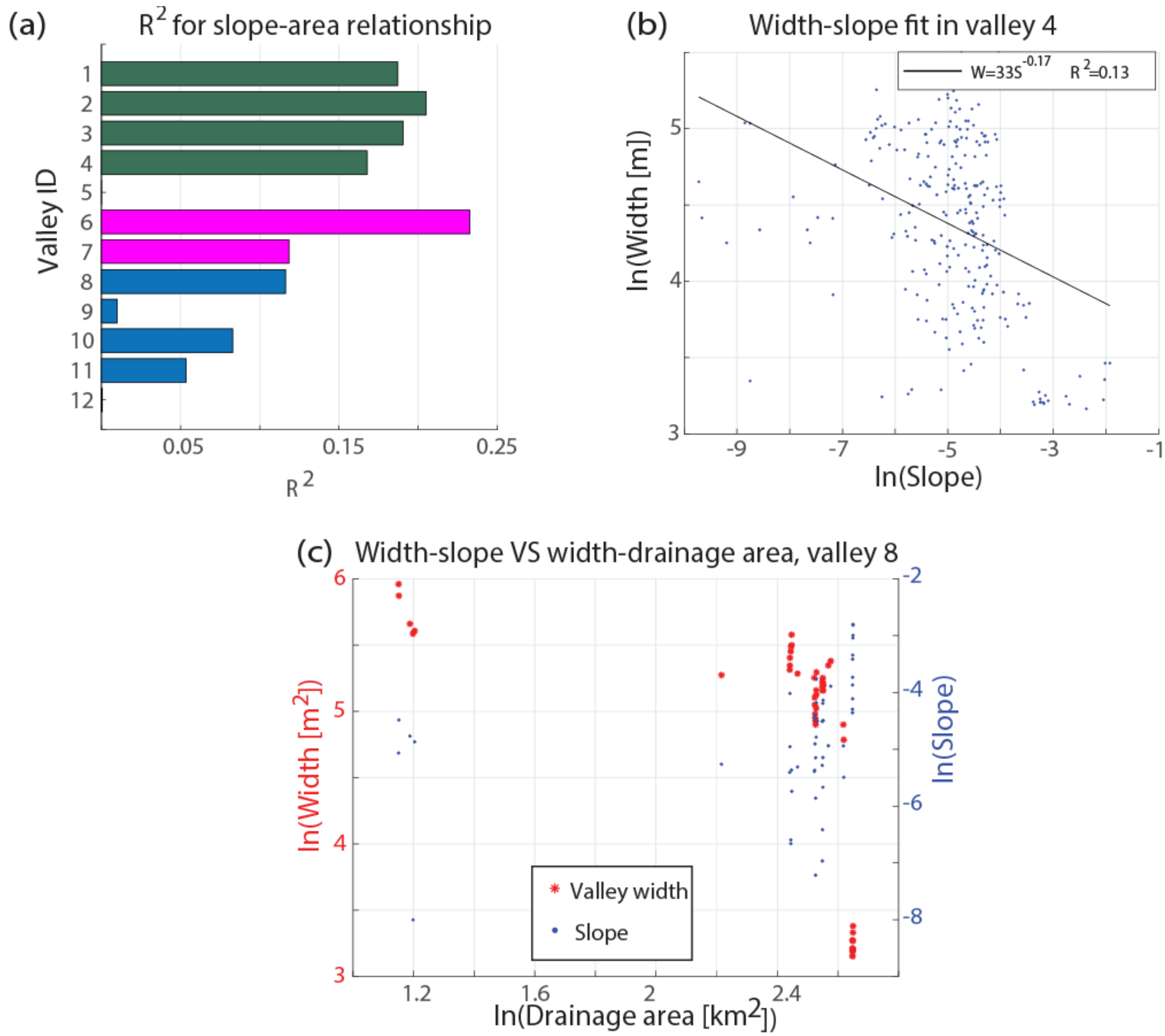

Figure S7 (a). R^2 values of slope-area regressions for the valleys in the study area. In valleys 5 and 12, R^2 is extremely small (>10-4) and thus is not visible. The bars are color-coded based on section category, where Green, pink, and blue are used for undisturbed (1-4), beheaded (5-7), and reversed (8-12), respectively. Overall, the R^2 values do not exceed 0.25, reflecting a poor correlation between slope and drainage area. (b) Width-slope relation along the undisturbed valley 4, illustrating the slope scatter that is present in the undisturbed and the beheaded categories. The black line represents a linear fit to the log-transformed width and slope, yielding a low R^2 of 0.13, likely resulting from the slope scatter. (c) Log-transformed width and slope plotted versus drainage area in the reversed valley 8. At the right edge of the graph, where the valley approaches the knickpoint, the valley narrows and the slope increases, such that the two parameters co-vary. We propose that narrowing and steepening are associated with flow acceleration above the knickpoint lip (Haviv et al., 2010).

Table S1: Parameters used in the ArcGIS tool 'VBET'- valley bottom extractor tool' (Gilbert et al., 2016) for the valleys in the study area

A full description of the VBET parameters is available in:

https://bitbucket.org/jtgilbert/riparian-condition-assessment-tools/wiki/Tool_Documentation/Version_1.0/VBET

Valleys ID	Minimal drainage area of flowlines	High drainage area threshold (km^2)	Low drainage area threshold (km^2)	Large slope threshold (degrees)	medium slope threshold	Small slope threshold	Large Buffer Size (m)	Medium Buffer Size (m)	Small Buffer Size (m)	Aggregation Distance (m)	Degree of manual editing: perimeter (%)[a]	Degree of manual editing: area (%)[b]
1,5	500	3	1	7	6	5	500	400	200	100	0	0
2,3	200	3	1	8	8	6	300	200	200	100	12.5	1.1
4	200	3	1	6	5	4	400	200	200	50	0	0
6,7	200	3	1	8	8	8	1000	500	100	100	0	0
8	200	2	1	8	8	3	400	200	200	100	12.3	2.7
9	500	12	0.1	10	5	3	200	200	400	100	11.5	4
10	50	4	0.1	14	14	14	300	200	200	100	1.1	0.3
11	50	4	0.1	14	14	14	300	200	200	100	10.1	4.7
12	50	3	0.1	6	6	15	300	200	250	50	23.8	9.4

[a]Calculated as: $x = \frac{|\text{polygon perimeter before editing} - \text{polygon perimeter after editing}|}{\text{polygon perimeter before editing}} * 100$

[b]Calculated as: $x = \frac{|\text{polygon area before editing} - \text{polygon area after editing}|}{\text{polygon area before editing}} * 100$

Table S2: Data used for producing Fig. 4, comparing TanDEM-X DEM based valley width relative to DGPS based width measurements.

TanDEM-X DEM based Width (m) [a]	DGPS-based width (m) [b]	Percent deviation, considering measurement errors [c]
30.31±16	10.9±0.6	25.5
74±16	84±1	0
113±16	108±1	0
129.78±16	113±1	0.3
140±16	119±3	0.2
144±16	124±3	0.3
204±16	202±2	0
RMSE [e] =13.1m		Mean: 3.7% Std.: 9.6%

[a]The DEM based width measurements were assigned with a constant error of $\sqrt{2} * R$, where R=11.6m (section 3.4 in the main text). The error was rounded to 16m.

[b]The DGPS-based width measurements error originate from the uncertainty of the distance between the sampling points along the transect (~1-2m).

[c]Percent deviation is calculated over the minimal difference between the TanDEM-X DEM based and the DGPS based measurements (i.e., widths measurements with overlapping errors are considered to have zero deviation), and calculated as: $\text{Percent deviation} = \frac{|\text{DEM width} - \text{DGPS width}|}{\text{DGPS width}} * 100$

[d]In transect 7, The DGPS measurement generated a profile with two channel bars. Given that the resolution of the TanDEM-X is not sufficient to capture such details, we manually smoothed the elevations across the bars to prevent their identification as the valley boundary.

[e]RMSE is based on the difference between the width extraction measurements without considering errors.

Table S3: P-values of the predictors and for the multivariate regressions

Channel ID	k_b coefficient P-value	b exponent P-value	c exponent P-value	Regression P-value
1	3.73E-83	7.82E-38	0.343801	4.16E-43
2	1.63E-99	1.15E-74	0.786131	1.24E-89
3	8.62E-127	8.24E-96	0.814645	9.68E-114
4	3.47E-95	4.18E-28	0.136348	8.44E-35
5	1.63E-68	6.51E-15	0.042025	1.62E-14
6	7.65E-64	1.29E-11	0.07223	7.36E-12
7	1.48E-98	5.30E-34	0.634481	6.97E-38
8	3.18E-10	0.002199	1.92E-09	1.16E-10
9	4.34E-07	0.003176	2.50E-05	2.64E-07
10	7.20E-14	1.20E-06	0.434009	2.87E-06
11	1.15E-09	2.26E-08	8.37E-10	1.16E-10
12	0.063748	0.000694	0.002154	7.50E-05

References

Dilts, T.E., 2015, Polygon to Centerline Tool for ArcGIS: University of Nevada Reno, http://www.arcgis.com/home/item.html?id=bc642731870740aabf48134f90aa6165.

Gabrish, G., 2020, Create Perpendicular Lines for ArcGIS.:, https://github.com/ShuksanGeomatics/Create_Perpendicular_Lines_ArcGIS.

Gilbert, J.T., Macfarlane, W.W., and Wheaton, J.M., 2016, The Valley Bottom Extraction Tool (V-BET): A GIS tool for delineating valley bottoms across entire drainage networks: Computers and Geosciences, v. 97, p. 1–14, doi: 10.1016/j.cageo.2016.07.014.

Haviv, I., Enzel, Y., Whipple, K.X., Zilberman, E., Matmon, A., Stone, J., and Fifield, K.L., 2010, Evolution of vertical knickpoints (waterfalls) with resistant caprock: Insights from numerical modeling: Journal of Geophysical Research: Earth Surface, v. 115, doi: https://doi.org/10.1029/2008JF001187.

Wessel, B., 2016, TanDEM-X Ground Segment – DEM Products Specification Document: EOC, DLR, Oberpfaffenhofen, Germany, Public Document TD-GS-PS-0021, Issue 3.1, https://tandemx-science.dlr.de/.